

# Amino functionalized hierarchically produced porous polyacrylamide microspheres for the removal of chromium(VI) from aqueous solution

Mehdi Karimi<sup>1</sup> · Ali Nematollahzadeh<sup>2</sup> · Akbar Shojaei<sup>1</sup>

Published online: 27 March 2017  
© Springer Science+Business Media New York 2017

**Abstract** Porous silica microspheres were used as hard template to produce porous polyacrylamide microspheres. The microspheres were modified with ethylenediamine and used for the removal of hexavalent chromium [Cr(VI)] from aqueous solution. Scanning electron microscopy, thermogravimetry analysis, and Fourier transform infrared spectroscopy were utilized to characterize the adsorbent. Adsorption of Cr(VI) was conducted in batch and dynamic modes, and effect of various parameters including solution pH, adsorbent dose, initial concentration of Cr(VI) and agitation time on the adsorption process was studied. The optimum pH for the maximum adsorption (124 mg Cr(VI)/g dry polymer) was found to be 3. Dynamic binding assay exhibited fast binding kinetics. The adsorption kinetics showed a good agreement with pseudo-second-order model. Meanwhile experimental data obtained from the batch binding assay could be well described by Langmuir isotherm model. The recovery of the adsorbent was successfully carried out by 0.2 M NaOH solution.

**Keywords** Amino functionalized · Polyacrylamide · Porous particle · Adsorption

## 1 Introduction

Nowadays the contamination associated with heavy metals is of great concern. The most hazardous heavy metals are arsenic, chromium, cadmium, mercury, zinc, lead, etc. Chromium is one of the most toxic heavy metals that can be introduced to environment by the variety of industrial effluents [1, 2]. Chromium exists in two oxidation states, hexavalent [Cr(VI)] and trivalent [Cr(III)]. Cr(III) is essential for microorganism in small quantities as a metal nutrient while hexavalent form is highly toxic so that nonstandard level of Cr(VI) in potable water can be significantly detrimental for human and other beings [3, 4]. Basically, the concentration of chromium in drinking water must be kept as low as possible, e.g. below 0.05 mg/L, to avoid any harmful effects on human body [5]. Therefore removal of heavy metal ions from the water resources has been the critical issue in both academia and industry.

In recent years, removal of chromium from aqueous solution has been the subject of many studies so various techniques have been introduced and their efficiencies have been examined. Conventional methods have been based on adsorption, membrane filtration, ion exchange, reverse osmosis, and electrochemical treatment methods [6]. Among the various methods, adsorption processes have shown many advantages like availability, cost-effectiveness, profitability, ease of operation, high efficiency and environmentally benign [6]. Various materials such as activated carbons [7], biomass [8], zeolites [9] have been examined as chromium sorbent. Among the organic materials, polyvinylpyridine [10], Polyacrylamide hydrogels [11], chitosan [12, 13] polyacrylonitrile fibers [14], polyaniline [3, 5] and polyethylene imine [15] have been widely exploited for removal of heavy metal ions from waste water.

---

✉ Ali Nematollahzadeh  
nematollahzadeha@uma.ac.ir

<sup>1</sup> Department of Chemical and Petroleum Engineering, Sharif University of Technology, Tehran, Iran

<sup>2</sup> Chemical Engineering Department, University of Mohaghegh Ardabili, P.O. Box 179, Ardabil, Iran

Polymeric porous beads with a large surface area and good pore interconnectivity are expected to have a large adsorption capacity and fast removal rate. These particles can be synthesized using a variety of methods such as suspension [16], dispersion [17] emulsion [18, 19] solvent evaporation [20] and precipitation polymerization [17]. In these techniques tuning the porosity and interconnectivity between pores as well as the size distribution of particles are very difficult or even impossible. In our previous works [21, 22], a new procedure to synthesize modified silica-polyacrylamide composite with spherical morphology was introduced and its capability was investigated in continuous removal of Cr(VI) and reactive black from the aqueous solution. In the present study, spherical porous polyacrylamide particles were prepared by washing out the silica constituent of above mentioned silica-polyacrylamide composite.

In this research, the adsorption capability of the porous polyacrylamide microspheres was investigated to remove Cr(VI) from the aqueous solution in batch mode processes. It is believed that polymeric porous particle, having larger surface area, is more efficient in adsorption processes. In order to enhance the adsorption capability and selectivity, the porous polymeric particles were post-treated by ethylenediamine.

## 2 Experimental procedures

### 2.1 Materials

Silica (Si1000, pore size 1000 Å, diameter 45–75 µm, pore volume 0.77 mL/g) was purchased from Silicycle (Canada). Acrylamide (AAm), *N,N'*-Methylene bisacrylamide (MBA), ammonium persulfate (APS), ethylenediamine, dimethylformamide (DMF), 2,2,4-trimethylpentane and potassium dichromate was purchased from Merck Chemical Company (Germany). Ammonium hydrogen difluoride was obtained from Acros (USA).

### 2.2 Synthesis and post treatment of adsorbent

To synthesize the polyacrylamide microspheres (PM), bare spherical silica particles were used as template. In the first step, silica-polyacrylamide microsphere composites were synthesized according to our previous work using a glass column [23]. Then the product (silica particle filled with polymer) was removed from the column and transferred into a plastic vial. Afterward the silica constituent was removed from the composite microsphere by dissolving in  $\text{NH}_4\text{HF}_2$  solution (3 M, 15 mL) for overnight at 20°C. After separating the liquid by centrifugation, the polymer microspheres were washed with distilled water until the pH reached 7 and then the particles were washed with 60 mL methanol ( $6 \times 10$  mL)

for dewatering. Finally the polymer particles were dried under vacuum at 60°C for 12 h (see Fig. 1). Treatment of the PM was performed with ethylene diamine (the sample was named MPM). Specified amount (2 g) of the PM sample was reacted with excess amount of ethylene diamine in round bottom flask equipped with a reflux condenser at 80°C for 9 h. Then the reaction mixture was poured into methanol and the MPM was separated via centrifugation. After that, MPM was washed with distilled water until the liquid became free of amine as traced by the absence of blue color with ninhydrin reagent. Eventually, the microspheres were washed with methanol and dried under vacuum at 40°C to get the final product.

With the same concentration of the monomers and the polymerization condition, bulk polymerization was also performed in a glass vial. The resultant bulk polymer was crushed and sieved to the size ranging from 45 to 75 µm (the sample was named BP). Modification of the BP was also performed with the same manner as mentioned above for the MPM sample. The modified BP sample was named MBP. The sample codes and descriptions are summarized in Table 1.

### 2.3 Characterization

Characterization of adsorbent was investigated with scanning electron microscopy (SEM, Hitachi-S4160) and Fourier transform infrared spectroscopy (ABB Bomem, MB-100 FTIR spectrophotometer). Prior to the SEM experiments, the particles were coated with gold and then the images were taken at 15.0 kV. Yield of the pore-filling process was determined by thermogravimetric analysis (TGA). TGA experiments were carried out in a TA instrument (Perkin Elmer STA 6000) using an open platinum pan at a heating rate of 10°C/min. The samples were heated up to 850°C at air atmosphere. The relative weight-losses (wt%) for the whole events were calculated by subtracting the weights between minima in the derivative plot and correcting this from minor weight loss due to dehydration of the bare silica.

### 2.4 Equilibrium percent swelling of polyacrylamide microspheres

Equilibrium swelling percent ( $P_s$ ) of PM and BP was determined by volumetric method. A specified amount of PM was placed in a glass tube with 5 mm internal diameter and 100 mm height. Then the glass tube was filled with distilled water and the equilibrium height of PM was measured. The  $P_s$  of PM was calculated from the following equation:

$$P_s(\%) = \frac{h_e - h_0}{h_0} \times 100 \quad (1)$$

where  $h_e$  and  $h_0$  are the equilibrium and initial heights of the microspheres in the glass tube respectively.

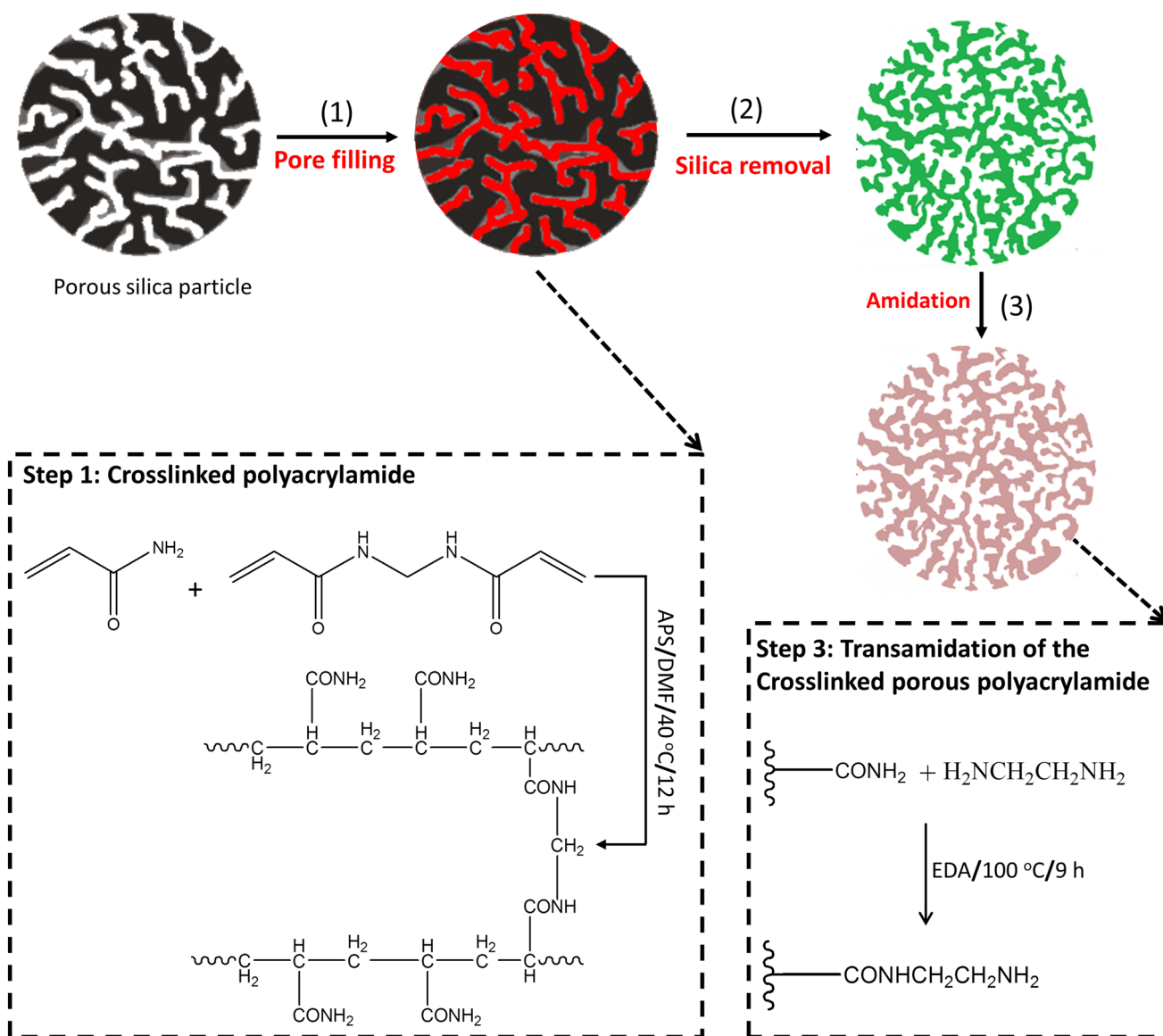


**Fig. 1** Schematic illustration of different steps used to produce porous PM

**Table 1** Sample codes and descriptions

Sample code	Description	Production method
PM	Polyacrylamide microspheres	Produced by polymerization in packed bed
MPM	Ethylenediamine modified PM	Amination reaction
BP	Polyacrylamide particles	Produced by bulk polymerization
MBP	Ethylenediamine modified BP	Amination reaction

**2.5 Adsorption experiments**

Chromium containing solutions were prepared by dissolving potassium dichromate in distilled water. All adsorption experiments were carried out in batch mode in 25 mL Erlenmeyer flask on a shaker at a shaking rate of 120 rpm

and temperature of 30 °C. The concentration of Cr(VI) was measured spectrophotometrically (Light wave WPA-S2000) at a wavelength of 540 nm using diphenyl carbazide method. To take into account the pH changes during the adsorption process, after the process, pH of the solution was

adjusted to the initial pH value and then the UV-absorbance was collected using UV/Vis- spectrophotometer.

To study the effect of solution pH on adsorption and to find an optimum pH (if any) for maximum adsorption, 10 mL of chromium solution with different initial concentrations (50, 100 and 150 mg/L) was added to 10 mg of the adsorbent. Solution pH (ranging from 2 to 6) was adjusted by aqueous HCl or NaOH solutions at 0.1–1 mol/L. With the optimum pH value in hand, the effect of initial Cr(VI) concentration (10–250 mg/L) was studied at the optimum pH. Dynamic binding assay was performed at two different initial concentrations of 50 and 100 mg Cr/L. Moreover the adsorbent dose was other variable that was studied at three different initial Cr(VI) concentrations (50, 100 and 150 mg/L). The adsorption percentage (A) of Cr(VI) was calculated from the following equation:

$$A(\%) = \frac{C_0 - C_e}{C_0} \times 100 \quad (2)$$

where  $C_0$  is the initial concentration of Cr(VI) solution (mg/L) and  $C_e$  is the free concentration of Cr(VI) in the binding solution after adsorption (mg/L) at equilibrium. Moreover the adsorption capacity of adsorbent can be calculated according to following equation:

$$q_e = \frac{(C_0 - C_e)V}{M} \quad (3)$$

where  $q_e$  is the adsorption capacity of adsorbent (mg/g, i.e. mg of Cr adsorbed per g of adsorbent),  $V$  is the volume of chromium solution (mL) and  $M$  is the mass of adsorbent (g).

## 2.6 Desorption study

To investigate the desorption capability of the particles, desorption process was carried out in batch mode. To do this, equilibrium adsorption was first performed at initial Cr(VI) concentration of 50 mg/L (10 mL) with 10 mg of the adsorbent for 20 min and at the optimum pH. The saturated adsorbent was separated from the solution by centrifugation and the solution was then analyzed for unbound Cr(VI) amount. The saturated adsorbent was transferred into 10 mL of various elution media including 0.2 M NaOH, 0.2 M HCl, 0.5 M NaCl and distilled water. Then the mixtures were agitated at 120 rpm and 30 °C for 20 min followed by centrifugation. The desorbed amount of Cr(VI) was determined by spectrophotometer. The percentage of desorption (D) was calculated from the following equation:

$$D(\%) = \frac{C_d}{C_0 - C_e} \times 100 \quad (4)$$

where  $C_0$  and  $C_e$  were already defined while  $C_d$  stands for the concentration of Cr(VI) in elution medium after desorption (mg/L).

## 3 Result and discussion

### 3.1 Characterization of adsorbent

The SEM microphotographs of silica and the produced polymer particles (Fig. 2) revealed that the procedure utilized for the production of polyacrylamide microspheres by using silica as sacrificial template was successful. The size distribution of polyacrylamide microspheres was also found to be similar with that of initial silica particles, i.e. 45–75  $\mu\text{m}$ .

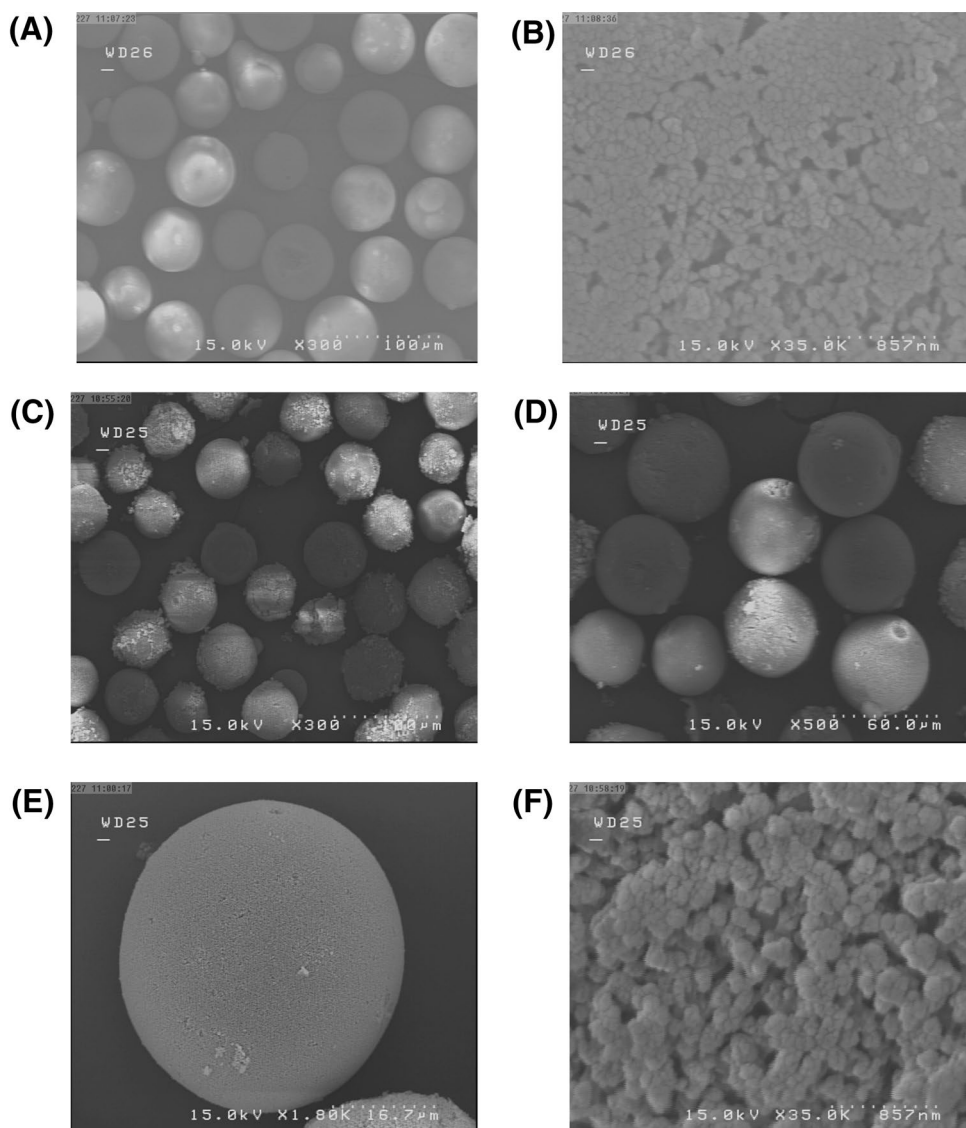
Infrared spectroscopy gives the useful information about the functional groups of adsorbent. FT-IR spectra of PM and MPM along with the MPM after adsorption of chromium are shown in Fig. 3. The FT-IR spectrum of PM (Fig. 3a) shows the common characteristic peaks for polyacrylamide. The characteristic bands of 3347 and 3197  $\text{cm}^{-1}$  are because of the N–H stretching vibrations. The bands at 2934 and 1449  $\text{cm}^{-1}$  are related to  $\text{CH}_2$  stretching vibrations. The pronounced peak appeared at 1655  $\text{cm}^{-1}$  is attributed to C=O group of amide I, absorption at 1412 and 1192  $\text{cm}^{-1}$  are assigned to deformation vibration of –NH groups and 1118  $\text{cm}^{-1}$  is related to C–N and N–H bonds (amide III) [24]. In the spectrum of polyacrylamide after the transamination reaction (MPM sample in Fig. 3b) a new peak at 1547  $\text{cm}^{-1}$  is observed which is related to secondary amide groups [11]. In short, the presence of this peak confirms the success of the transamination reaction. As can be seen in Fig. 3c, after adsorption of chromium, the peak at 1547  $\text{cm}^{-1}$  is disappeared and two new peaks at 939 and 881  $\text{cm}^{-1}$  are observed which are attributed to Cr–O and Cr=O bonds from the Cr(VI) species.

Thermogravimetric analysis was applied to determine the yield of the pore-filling process. Using TGA thermograph of the composite adsorbent (Fig. 4) and also the theoretical mass of polymer loaded in the pores of silica, the pore-filling yield was calculated through the following equation:

$$\text{Pore filling yield} = \frac{\text{Sample weight loss in TGA/g of silica}}{\text{Theoretical weight of polymer/g of silica}} \times 100 \quad (5)$$

Taking into account the pore volume of the silica (0.77 cc/g), the theoretical weight of the polymer in the pores of silica was about 308 mg/g of silica. Hence, according to the TGA result the sample weight loss of ca.

**Fig. 2** SEM micrograph of **a** silica particles, **b** surface of a silica particle, **c**, **d** polymer particles, **e** single polymer particle and **f** surface of a polymer particle



283 mg/g of silica (i.e. 78.85%) yields 92% pore filling efficiency for the presented method. This shows the success of the adopted method for the intrusion of the polymerization solution into the pores of the silica microspheres. The yield less than 100% is probably due to imperfect penetration of the polymerization solution mainly into the nanopores (i.e. pore size <2 nm) [22, 23].

### 3.2 Equilibrium percent swelling

Using Eq. (1), the equilibrium swelling of PM and BP was found to be 300 and 200%, respectively. Actually, the swelling ratio of both particles, i.e. PM and BP, is relatively low which can be ascribed to their high degree of crosslinking with 10 wt% crosslinker. However, comparatively higher swelling percent of PM with respect to BP can be associated to its porous structure with well-connected pores

enabling the absorption of higher content of water into the particle.

### 3.3 Batch binding experiments

#### 3.3.1 Effect of pH on adsorption

Solution pH has a considerable effect on the speciation of Cr(VI) as well as surface charge of the adsorbent. Therefore, the adsorption would be strongly pH dependent. Depending on solution pH, various forms of chromium anion such as  $\text{HCrO}_4^-$ ,  $\text{HCr}_2\text{O}_7^-$ ,  $\text{CrO}_4^{2-}$ , and  $\text{Cr}_2\text{O}_7^{2-}$  could be present. Figure 5 exhibits the influence of solution pH on the adsorption capacity of MPM. It is revealed that regardless of initial concentration of Cr(VI), the maximum removal of Cr(VI) is achieved at pH=3 which was opted as optimum pH for the rest of adsorption

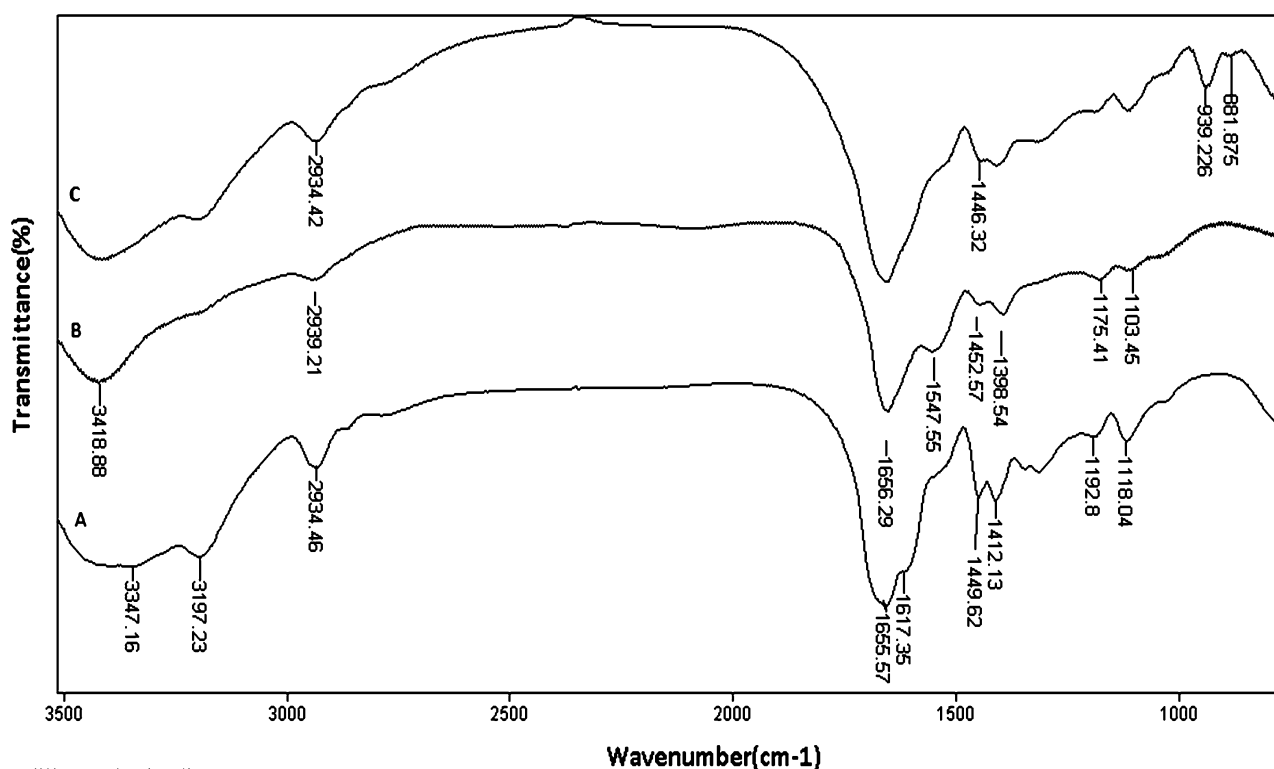


**Fig. 3** FT-IR spectra of **a** adsorbent before amination (PM), **b** adsorbent after amination (MPM), **c** MPM after chromium adsorption

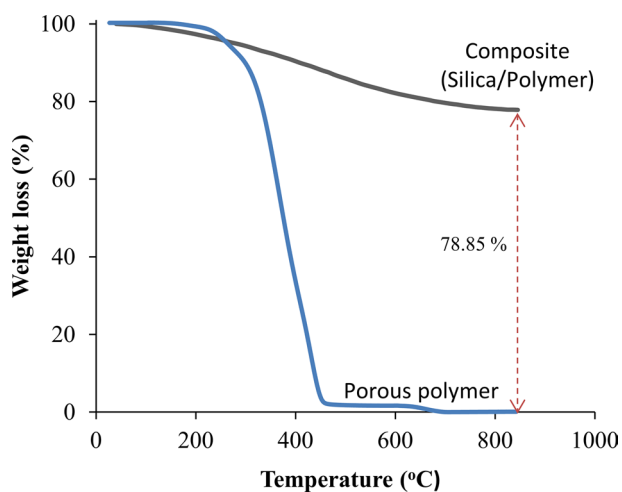


**Fig. 4** TGA thermographs of composite and hierarchically produced porous polymer

experiments. It is obvious that at low pH values, amine groups of adsorbent become protonated and consequently electrostatic attraction between chromium anions and positive amine groups of the adsorbent become responsible for high removal of Cr(VI). In addition to adsorption process, reduction of Cr(VI) to Cr(III), which is much probable under acidic condition, can be considered as an extra

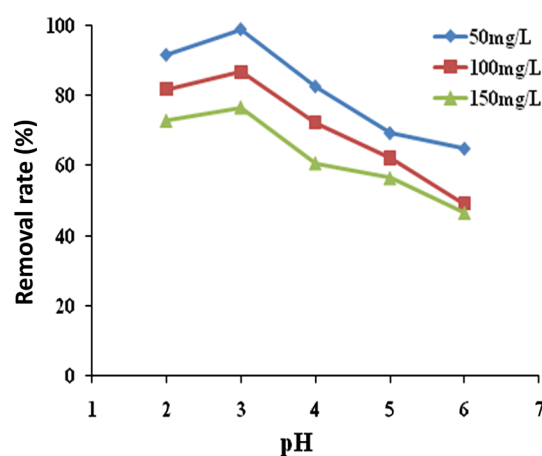


**Fig. 5** Effect of pH on degree of adsorption of Cr(VI) (conditions: initial concentration of Cr(VI) 50, 100, 150 mg/L; MPM dose 1 g/L; agitation time 20 min and agitation speed 120 rpm)

source for excess removal of Cr(VI) [3, 23] at low pH values. However, at very acidic condition, i.e. pH values as low as 1, the concentration of  $\text{H}_2\text{CrO}_4$  increases according to the following equilibrium reaction:

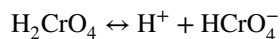


**Table 2** Effect of initial Cr(VI) concentrations on degree of adsorbent (MPM) capacity (conditions: pH=3; MPM dose 1 g/L; agitation time 20 min and agitation speed 120 rpm)

Initial concentration (mg/L)	10	30	50	70	100	150	200	250
q <sub>e</sub> (mg/g)	9.8	29.4	49.3	65.6	87.0	116.1	111.6	123.9

**Table 3** Comparison between different adsorbents on adsorption of Cr(VI)

Adsorbent	Maximum adsorption capacity (mg/g)	Optimum pH	Equilibrium time (h)	Refs.
Hazelnut shell activated carbon	170	1	72	[26]
Activated carbon from Heveabrasillinesis saw dust	44.1	2	5	[27]
Activated carbon	3.46	3	3	[28]
Chitosan cross-linked with epichlorohydrin	11.3	3	0.13	[29]
Polyaniline–poly ethylene glycol composite	68.97	5	0.5	[3]
Ethylenediamine-modified cross-linked magnetic chitosan resin	51.8	2	0.1–0.166	[30]
Diatomite-supported magnetite nanoparticles	69.16	2	1	[31]
Nanocrystallineakaganeite	79.66	5.5	1	[32]
Hydrous zirconium oxide	61	2	1	[33]
Polypyrrole/wood sawdust	3.4	5	0.16	[34]
Polyacrylamide-grafted sawdust	45	3	2	[4]
Modified silica-polyacrylamide microspheres composite	57.78	3	–	[21]
Modified polyacrylamide microspheres	124	3	0.33	Present study

Accordingly, a decrease in adsorption is expected at this condition due to less electrostatic attraction between the adsorbent and chromium. At pH values above 3 the surface of adsorbent becomes less positive and furthermore, the concentration of OH<sup>-</sup> ions in the medium increases. Therefore, the chromium species and the hydroxyl ions compete for the positive sites of the adsorbent. Hence, removal of Cr(VI) begins to decrease with increase of pH above 3.

To compare the MPM with MBP, the adsorption experiment was carried out by addition of the MBP (at concentration of 1 g/L) to 50 mg/L of chromium solution at the optimum pH value of 3. The result showed 89.1% removal of Cr(VI) that is almost 10% lower than the adsorption efficiency of MPM in the same condition. Such difference can be attributed to the higher surface area of MPM which is due to its higher interior surface inside the pore structure. It is also assumed that the interior surface of MPM is completely amine modified during modification. These make possible more adsorption of Cr(VI) for MPM.

3.3.2 Effect of initial concentration of Cr(VI) and MPM dose on Cr(VI) adsorption

The effect of initial concentration of Cr(VI) on the degree of adsorption was investigated at eight different initial Cr(VI) concentrations ranging from 10 to 250 mg/L. The results are presented in Table 2 and

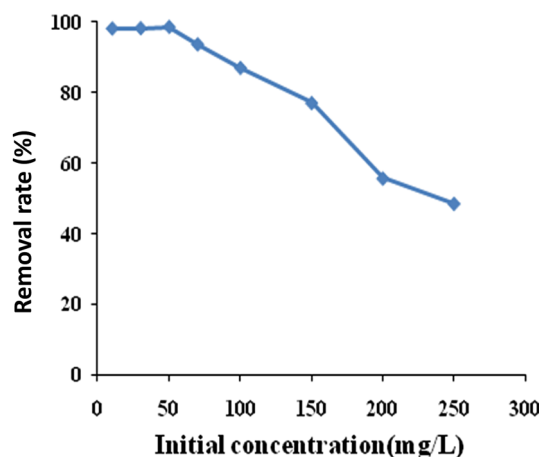


**Fig. 6** Effect of initial concentration of Cr(VI) on degree of adsorption (conditions: pH 3; MPM dose 1 g/L; agitation time 20 min and agitation speed 120 rpm)

Fig. 6. It is observed that with increasing the initial concentration from 10 to 250 mg/L, the degree of adsorption increases from 9.82 to 123.99 mg/g while the percentage of adsorption decreases from 98.2 to 48.6%. The comparison between equilibrium adsorption capacity and the corresponding equilibrium time for present adsorbent with some other Cr(VI) adsorbents reported in literature is given in Table 3. Comparatively, MPM

presented in this study shows the greater capacity for removal of Cr(VI) as well as the faster adsorption process. As can be seen in Table 3, compared with modified silica-polyacrylamide composite reported in our previous work [21], the present modified porous polyacrylamide microspheres show larger adsorption capacity, as large as 2.15-folds. Some types of active carbon have shown the large capacity for removal of Cr(VI) but their adsorption kinetics is very slow. Furthermore, regeneration of active carbon usually affects the properties of the carbon and makes it less effective for reuse [25].

Figure 7 exhibits the influence of MPM dose on the degree of adsorption of Cr(VI) at three initial concentrations of Cr(VI). As can be seen, degree of adsorption increases with increasing the adsorbent dosage from 0.2 to 1 g/L. Beyond 1 g/L no significant increment in removal of Cr(VI) is observed and degree of adsorption increases very marginally which is consistent with literature reports [34–37]. Reaching to equilibrium between metal ions and adsorbent at the operating conditions and overcrowding of adsorbent particles at high concentrations of solid phase are probably responsible for this behavior [36]. Interestingly, high level of Cr(VI) was able to be removed even at a few amount of MPM. For instance, at initial Cr(VI) concentration of 50 mg/L, 85 and 94% Cr(VI) removal occurred only with 0.2 and 0.5 g/L of adsorbent, respectively. High porosity and good interconnectivity between pores of the microspheres, which facilitate the diffusion of Cr(VI) ions into interior surface of the adsorbent, were expected to be responsible for such behavior.

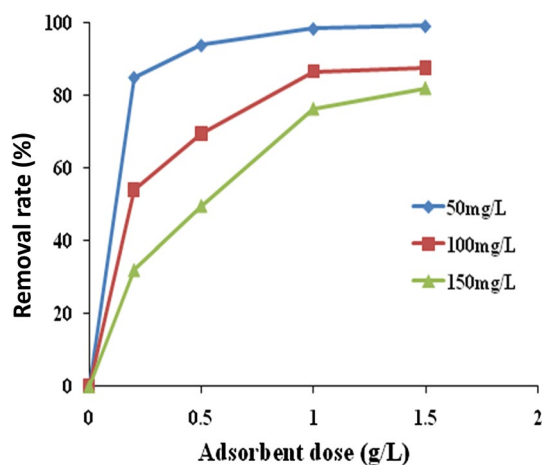


**Fig. 7** Effect of adsorbent (MPM) dose on degree of adsorption Cr(VI) (conditions: initial Cr(VI) concentration 50, 100, 150 mg/L; pH 3; agitation time 20 min and agitation speed 120 rpm)

### 3.3.3 Effect of agitation time on adsorption and kinetic models

Adsorption kinetic by MPM was studied at two different Cr(VI) initial concentrations of 50 and 100 mg/L. As shown in Fig. 8, major portion of Cr(VI) removal has occurred in first 5 min. The adsorption of Cr(VI) increased with time, however, there was no significant change in the adsorption process after about 20 min. This suggests a very fast adsorption process for MPM. For instance at initial concentration of 50 mg/L, 70 and 93% removal occurred within 2 and 10 min, respectively. This can be attributed to high accessible exposed surface area of polymeric porous microspheres originated basically from good interconnectivity of the pores.

In order to obtain a deep insight into the adsorption mechanisms of Cr(VI) in our system, the adsorption kinetic was investigated based on the pseudo-first and pseudo-second order models. The linearized form of the pseudo-first-order and pseudo-second-order models [38] is given by Eqs. 6 and 7, respectively, as follows:

$$\log(q_e - q_t) = \log q_e - \frac{kt}{2.303} \quad (6)$$

$$\frac{t}{q_r} = \frac{1}{k'q_e^2} + \frac{t}{q_e} \quad (7)$$

where  $q_e$  is the amount of metal ions adsorbed at equilibrium (mg/g),  $q_t$  is the amount of metal ions adsorbed by MPM at time  $t$  (mg/g),  $k$  and  $k'$  ( $\text{min}^{-1}$ ) are the constants. Values of  $q_e$  and  $k$  can be obtained from slope and intercept, respectively, of the plot  $\log(q_e - q_t)$  versus time for pseudo-first-order, as shown in Fig. 9a. Similarly,

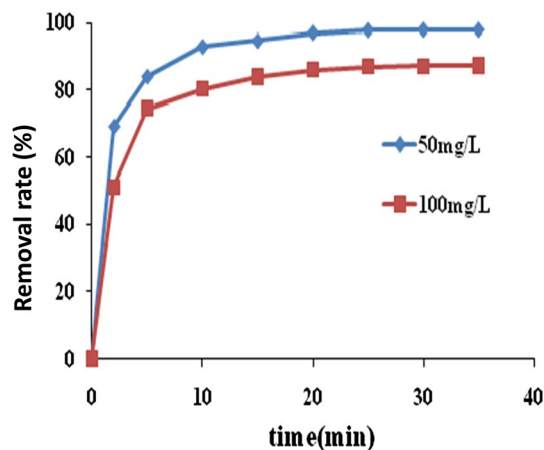


**Fig. 8** Effect of agitation time on degree of adsorption (conditions: initial Cr(VI) concentration 50, 100 mg/L; pH 3; MPM dose 1 g/L and agitation speed 120 rpm)



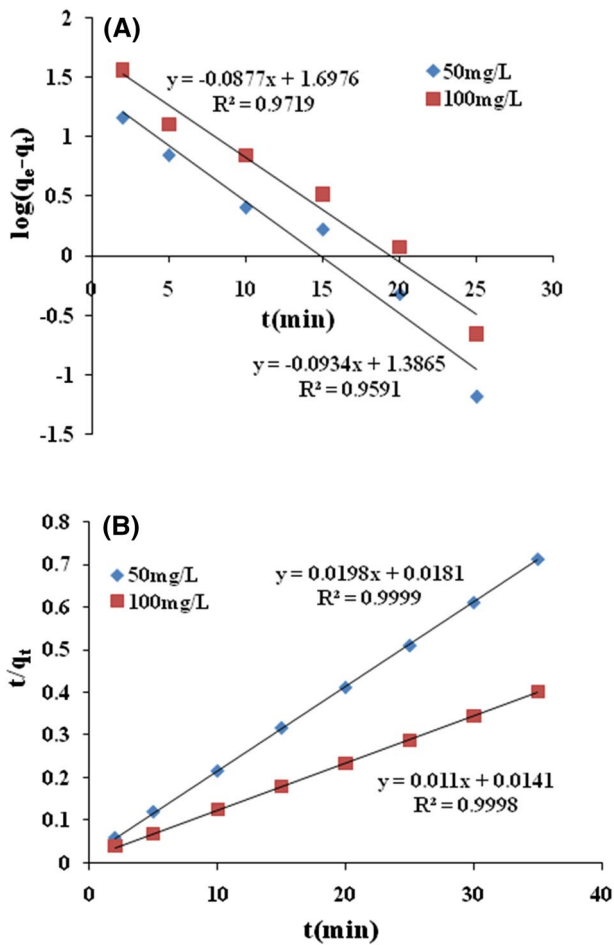


**Fig. 9** **a** Pseudo-first-order model at two different initial concentrations of Cr(VI), **b** Pseudo-second-order model for two different initial concentrations of Cr(VI) (conditions: pH 3; MPM dose 1 g/L; agitation time 20 min and agitation speed 120 rpm)

values of  $q_e$  and  $k'$  for pseudo-second-order model can also be obtained from slope and intercept of  $t/q_t$  versus  $t$  (see Fig. 9b). As can be inferred, experimental data does not show a good correlation with pseudo-first-order model and the model prediction exhibits a large deviation from experimental data (see Table 4). However, the pseudo-second-order shows a very good correlation. This suggests that the capacity of adsorbent is proportional to the number of active sites on the surface illustrating

monolayer adsorption of adsorbent on the surface [38]. Additionally, it can be concluded that the chemisorptions governs the adsorption process in this polymeric porous particles [39].

### 3.4 Adsorption isotherms of Cr (VI)

The adsorption equilibrium data obtained at 30 °C, pH=3 and initial Cr(VI) concentrations in the range of 10–250 mg/L were used to construct adsorption isotherms. Two common isotherms, i.e. Langmuir and Freundlich, were used. The linearized form of the Langmuir (Eq. 8) and Freundlich (Eq. 9) isotherms are expressed as follows:

$$\frac{C_e}{q_e} = \frac{1}{K_f q_{max}} + \frac{C_e}{q_{max}} \tag{8}$$

$$\log q_e = \frac{1}{n} \log C_e + \log K_f \tag{9}$$

where  $C_e$  is the equilibrium Cr(VI) concentration (mg/L),  $q_e$  is the equilibrium amount of solute adsorbed per unit mass of adsorbent (mg/g),  $q_{max}$  is the maximum quantity of metal ions per unit mass of adsorbent to form a complete monolayer on the surface of adsorbent (mg/g),  $K_f$  is the Langmuir constant related to free adsorption energy (L/mg), and  $K_f$  and  $n$  are the Freundlich constants indicating adsorption capacity and intensity, respectively. The plots of  $C_e/q_e$  versus  $C_e$  and  $\log q_e$  versus  $\log C_e$  give the Langmuir and Freundlich constants. It should be noted that the difference between Langmuir and Freundlich isotherms comes from their assumption wherein the Langmuir isotherm accounts for the surface as homogeneous while Freundlich model considers it as heterogeneous medium. The adsorption isotherms are shown in Fig. 10a, b, and the isotherms constants are listed in Table 5. The results show that the adsorption of Cr(VI) onto the adsorbent can be well fitted in Langmuir isotherm but Freundlich model did not show a good correlation. Therefore Langmuir isotherm is more suitable for this adsorbent justifying the monolayer adsorption process onto the surface, with finite number of identical sites, which are homogeneously distributed over the adsorbent surface.

**Table 4** Kinetic parameters obtained from pseudo-first-order and pseudo-second-order models (conditions: pH 3; MPM dose 1 g/L; agitation time 20 min and agitation speed 120 rpm)

$C_0$ (mg/L)	$q_{e (exp.)}$ (mg/g)	Pseudo-first-order model			Pseudo-second-order model		
		$K$ ( $\text{min}^{-1}$ )	$q_{e (cal.)}$ (mg/g)	$R^2$	$K'$ ( $\text{min}^{-1}$ )	$q_{e (cal.)}$ (mg/g)	$R^2$
50	49.3	0.21	23.9	0.959	$0.21 \times 10^{-1}$	50.5	0.999
100	87	0.20	49.8	0.971	$0.86 \times 10^{-2}$	90.9	0.999

**Fig. 10** **a** Langmuir **b** Freundlich isotherm for Cr(VI) adsorption (conditions:  $C_0=10, 30, 50, 70, 100, 150, 200, 250$  mg Cr(VI) /L; pH 3; MPM dose 1 g/L; temperature 30 °C; agitation time 20 min and agitation speed 120 rpm)

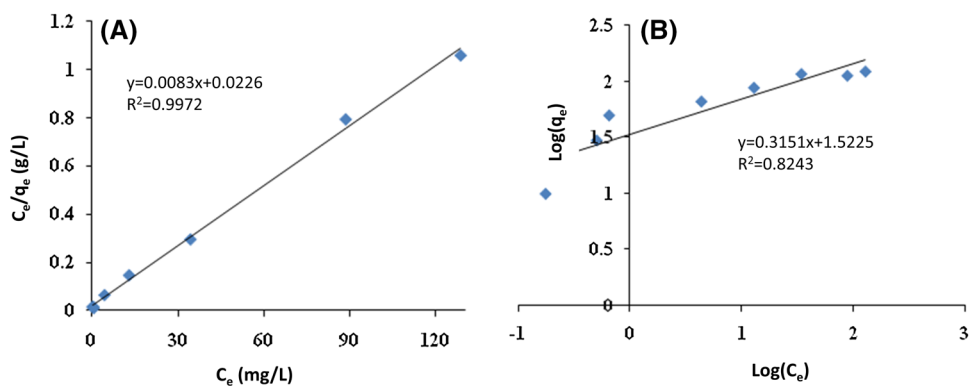


**Table 5** Langmuir and Freundlich isotherms constants (conditions:  $C_0=10, 30, 50, 70, 100, 150, 200, 250$  mg Cr(VI) /L; pH 3; MPM dose 1 g/L; temperature 30 °C; agitation time 20 min and agitation speed 120 rpm)

Langmuir isotherm		Freundlich isotherm	
$k_l$	$q_{max}$ (mg/g)	$k_f$	$n$
0.367	120.48	33.3	3.17

### 3.5 Desorption study

Desorption study was carried out in four elution media including 0.2 M NaOH, 0.2 M HCl, 0.5 M NaCl and distilled water. The degree of desorption with distilled water was <1% while the desorption rate with 0.2 M NaOH, 0.2 M HCl and 0.5 M NaCl were found to be 92.35, 78.95 and 78.75%, respectively. This suggests that 0.2 M NaOH solution is much successful in regeneration of MPM adsorbent.

## 4 Conclusions

The application of novel amino functionalized porous polyacrylamide microspheres as adsorbent of Cr(VI) from aqueous solution was investigated. The adsorption study showed that MPM is able to remove Cr(VI) from aqueous solution in a great amount and in a very fast process. The adsorbent capacity at optimum pH, i.e. pH=3, was found to be 123.9 mg of Cr(VI) ions per 1 g of MPM at initial concentration of 250 mg/L which was significantly high in comparison with many other adsorbents reported in literature. It was shown that the high Cr(VI) removal occurred even at low amount of adsorbent, so 85% Cr(VI) was removed with only 0.2 g/L adsorbent in initial Cr(VI) concentration of 50 mg/L. The pseudo-second-order model could describe the adsorption kinetic appropriately and equilibrium data was also in good agreement with Langmuir isotherm. The main mechanism for adsorption of Cr(VI) by adsorbent was speculated to be the electrostatic forces as well as the chemical interaction between chromium and adsorbent. The

results suggested that the porous polymeric microspheres synthesized in this study could be an efficient adsorbent for removal of Cr(VI) from aqueous solution.

**Acknowledgements** This work was supported by the research vice presidency of Sharif University of Technology and Iranian nanotechnology initiative council. Their supports are greatly appreciated.

## References

- L.V.A. Gurgel, J.C. Perin de Melo, J.C. de Lena, L.F. Gil, *Bioreour. Technol.* **100**, 3214–3220 (2009)
- M. Owlad, M.K. Aroua, W.M.A. Wan Daud, *Bioreour. Technol.* **101**, 5098–5103 (2010)
- M.R. Samani, S.M. Borghei, A. Olad, M.J. Chaichi, *J. Hazard. Mater.* **184**, 248–254 (2010)
- C. Raji, T.S. Anirudhan, *Water Res.* **32**, 3772–3780 (1998)
- P.A. Kumar, S. Chakraborty, M. Ray, *Chem. Eng. J.* **141**, 130–140 (2008)
- M. Owlad, M.K. Aroua, W.A.W. Daud, S. Baroutian, *Water Air Soil Pollut.* **200**, 59–77 (2009)
- D. Mohan, C.U. Pittman Jr., *J. Hazard. Mater.* **137**, 762–811 (2006)
- A.U. Kurikka, V.P.M. Shafi, A. Dyal, X.Z. Yan, N.L. Yang, C. Estourne's, L. Fourne's, A. Wattiaux, H. White, M. Rafailovich, *Chem. Mater.* **14**, 1778–1787 (2002)
- D. Wu, Y. Sui, S. He, X. Wang, C. Li, H. Kong, *J. Hazard. Mater.* **155**, 415–423 (2008)
- D. Gang, S.K. Banerji, T.E. Clevenger, *Practice periodical of hazardous, toxic, and radioactive. Waste Manag.* **4**, 105–110 (2000)
- H. Kaşgöz, S. Özgümüş, M. Orbay, *Polymer* **42**, 7497–7502 (2001)
- G. Rojas, J. Silva, J.A. Flores, A. Rodriguez, M. Ly, H. Maldonado, *Sep. Purif. Technol.* **44**, 31–36 (2005)
- Y.M. Hao, C. Man, Z.B. Hu, *J. Hazard. Mater.* **184**, 392–399 (2010)
- S. Deng, R. Bai, *Water Res.* **38**, 2424–2432 (2004)
- A. Denizli, S. Senel, G. Alsancak, N. Tüzmen, R. Say, *React. Funct. Polym.* **55**, 121–130 (2003)
- J.-H. Yeum, Y. Deng, *Colloid Polym. Sci.* **283**, 1172–1179 (2005)
- K. Saralidze, L.H. Koole, M.L.W. Knetsch, *Materials* **3**, 3537 (2010)
- M. Okubo, Y. Yamamoto, S. Kamei, *Colloid Polym. Sci.* **267**, 861–865 (1989)

19. E. Pollert, K. Knížek, M. Maryško, K. Závěta, A. Lančok, J. Boháček, D. Horák, M. Babič, J. Magn. Magn. Mater. **306**, 241–247 (2006)
20. P.B. O'Donnell, J.W. McGinity, Adv. Drug Delivery. Rev. **28**, 25–42 (1997)
21. M. Karimi, A. Shojaei, A. Nematollahzadeh, M.J. Abdekhodaie, Chem. Eng. J. **210**, 280–288 (2012)
22. A. Nematollahzadeh, A. Shojaei, M. Karimi, React. Funct. Polym. **86**, 7–15 (2015)
23. A. Nematollahzadeh, W. Sun, C.S.A. Aureliano, D. Lütkemeyer, J. Stute, M.J. Abdekhodaie, A. Shojaei, B. Sellergren, Angew. Chem. Int. Ed. **50**, 495–498 (2011)
24. H. Kaşgöz, S. Özgümüş, M. Orbay, Polymer **44**, 1785–1793 (2003)
25. J. Hu, G. Chen, I.M.C. Lo, Water Res. **39**, 4528–4536 (2005)
26. M. Kobya, Bioresour. Technol. **91**, 317–321 (2004)
27. T. Karthikeyan, S. Rajgopal, L.R. Miranda, J. Hazard. Mater. **124**, 192–199 (2005)
28. K. Selvi, S. Pattabhi, K. Kadirvelu, Bioresour. Technol. **80**, 87–89 (2001)
29. S. Qian, G. Huang, J. Jiang, F. He, Y. Wang, J. Appl. Polym. Sci. **77**, 3216–3219 (2000)
30. X.-J. Hu, J.-S. Wang, Y.-G. Liu, X. Li, G.-M. Zeng, Z.-l. Bao, X.-X. Zeng, A.-W. Chen, F. Long, J. Hazard. Mater. **185**, 306–314 (2011)
31. N.K. Lazaridis, D.N. Bakoyannakis, E.A. Deliyanni, Chemosphere **58**, 65–73 (2005)
32. L.A. Rodrigues, L.J. Maschio, R.E. da Silva, M.L.C.P. da Silva, J. Hazard. Mater. **173**, 630–636 (2010)
33. R. Ansari, N.K. Fahim, React. Funct. Polym. **67**, 367–374 (2007)
34. L.J. Yu, S.S. Shukla, K.L. Dorris, A. Shukla, J.L. Margrave, J. Hazard. Mater. **100**, 53–63 (2003)
35. P.A. Kumar, M. Ray, S. Chakraborty, J. Hazard. Mater. **143**, 24–32 (2007)
36. N.R. Bishnoi, M. Bajaj, N. Sharma, A. Gupta, Bioresour. Technol. **91**, 305–307 (2004)
37. K. Mohanty, M. Jha, B.C. Meikap, M.N. Biswas, Chem. Eng. Sci. **60**, 3049–3059 (2005)
38. Y.S. Ho, G. McKay, Process Saf. Environ. Prot. **76**, 183–191 (1998)
39. X. Luo, S. Luo, Y. Zhan, H. Shu, Y. Huang, X. Tu, J. Hazard. Mater. **192**, 949–955 (2011)